Published in IET Microwaves, Antennas & Propagation
Received on 23rd February 2010
Revised on 20th May 2010
doi: 10.1049/iet-map.2010.0070

ISSN 1751-8725

Effects of interface conditions and long-term stability of passive intermodulation response in printed lines

A.P. Shitvov[1] T. Olsson[2] J. Francey[3] D.E. Zelenchuk[1]
A.G. Schuchinsky[1] B. El Banna[4]

[1]The Institute of Electronics, Communications and Information Technology (ECIT), Northern Ireland Science Park, Queen's University of Belfast, Queen's Road, Queen's Island, Belfast BT3 9DT, Northern Ireland, UK
[2]Powerwave Technologies Sweden AB, Knarrarnasgatan 7 8tr., Kista 164 40, Sweden
[3]Taconic Advanced Dielectric Division, Mullingar Business Park, Mullingar, Co. Westmeath, Republic of Ireland
[4]Laird Technologies, Kryptongatan 20, Mölndal SE-431 63, Sweden
E-mail: a.shitvov@qub.ac.uk

Abstract: An experimental investigation of the effect of conductor-to-substrate interface on distributed passive intermodulation (PIM) generation in printed microstrip lines has been undertaken using the custom-designed microwave laminates with removed surface bonding layers and with the commercial adhesion promotion applied to the conductor underside. The study of long-term stability of PIM performance of the printed circuits is reported for the first time. The comprehensive measurement results, observations of the self-improvement of the PIM performance and the effect of panel bending on PIM generation in printed boards with different finishing are presented. A consistent physical interpretation of the observed phenomena is proposed. The results of this study provide new important considerations for the design and characterisation of low-PIM printed circuits.

1 Introduction

Passive intermodulation (PIM) in printed circuit boards (PCBs) has been a subject of extensive industrial and academic research since the early days of application of PCBs in printed antennas, phased arrays, power combiners, filters and other high performance components of the communications systems and radars [1–4]. The PCBs are increasingly employed in the modern electronic equipments, ranging from the mobile phone base stations to the spacecraft communication and navigation payloads, where integrity of the complex modulated signals is paramount. The use of the integrated radio frequency (RF) front-ends, including high-power multi-channel transmitters, sensitive receivers and shared or co-located antennas, imposes extremely stringent requirements to the PIM performance of the PCB-based devices. The detrimental effect of PIM generation by the printed components is forewarned for the next generation of emerging broadband wireless communications [5].

Although the system requirements to the PIM performance of RF front-end vary with the type of services, it is a common practice in industry that the maximum allowable level of the reflected third-order PIM product in the receive band of GSM900 antennas must not exceed −107 dBm at 2 × 43 dBm CW carriers located in the transmit band [6]. This figure is determined by the GSM900 receiver sensitivity and maximum allowed interference level specified by GSM 05.05 standard [7]. In the absence of the established industrial standards on PIM characterisation of printed circuits and components, microwave material and antenna manufacturers commonly employ the two-tone PIM testing, in which the device under test (antenna) is fed with two continuous wave (CW) carriers of 43 dBm each, separated in frequency to

produce the PIM products within the receive band of a given communication services [6–8].

Recently, a series of investigations have been undertaken to identify the principal mechanisms and sources of PIM production in printed lines fabricated on commercial microwave laminates [9–13]. It has been shown that the weak distributed non-linearities inherent to the conductor cladding and material of the dielectric substrate are the major contributors to PIM generation in PCB [14]. The distributed non-linearity of the conductor cladding has been attributed to the material and quality of finish coating, fractured edges of etched tracks, conductor-to-substrate interface roughness and contamination [9]. The substrate non-linearity is usually associated with the base dielectric composition and surface bonding layers [15, 16]. Although the impact of certain structural parameters of the laminates on their PIM performance has been addressed in the literature, the effect of interface between the dielectric and conductor cladding requires further investigation. This particularly concerns the materials with commercial copper treatment, widely employed to improve the conductor-to-substrate adhesion. Long-term stability of PIM performance of the processed PCBs represents another important issue that, to the authors' knowledge, has not been addressed in the technical literature yet.

This paper reports on the experimental study of the conductor-to-dielectric interface contribution to the distributed PIM generation and stability of the PIM performance of the processed printed circuits. The experimental methodology is based on the two-port forward/reverse PIM measurements [17]. The effect of the interface condition is analysed in Section 2 by comparison of the PIM responses of several microstrip lines with modified interfaces. The long-term stability of the PIM performance, discussed in Section 3, has been investigated using the laminates with different finishing. A consistent interpretation of the observed effects has been proposed and the practical implications of the obtained results are discussed. The main findings are summarised in conclusions.

2 Effect of the conductor-to-substrate interface

From the physical standpoint, the distributed non-linearity of printed lines represents the collective response of a continuum of microscopic non-linearities. Each of the non-linearities presents a 'spot source' causing isotropic non-linear scattering of the fundamental tones with a number of physical phenomena engaged in the process. The spatial scale of the local scattering may vary from the barrier length associated with the tunnelling through the oxide layers and carriers transport across the grain boundaries of polycrystalline conductors to the size of a ferroic domain or microscopic voids at the fractured strip edges and at rough interface with the scale determined by the size of a copper dendrite [9]. While the distributed microscopic structural defects are responsible for the PIM production in printed transmission lines, they are commonly characterised by the macroscopic quantities, depending on the physical nature of non-linearity, for example, by non-linear surface impedance, bulk conductivity and so on [14].

In the ordinary printed circuits, operating at ambient temperatures, conductor-to-substrate interface often makes a significant contribution to the PIM production. To investigate this phenomenon, a series of experiments with the on-purpose built laminates has been performed using the test setups described in [17]. Details of the microstrip layouts and the contactless test fixture can be found in [10, 11]. Suffice it to note here only that two different types of the microstrip launchers have been employed in the two-port PIM measurements: direct cable microstrip launchers (DCL) and contactless broadside strip launchers (CSL). Even though these two approaches are consistent, the measurement results presented below are analysed separately with the reference to the individual test setups.

Fig. 1 shows the comparison of the PIM responses of three laminates which differ only in the conductor-to-substrate interface. Two-port measurements of the forward and reverse third-order passive intermodulation (PIM3) products (intermodulation frequency $f_{PIM3} = 2f_1 - f_2$, where $f_{1,2}$ are the fundamental tones) have been performed on 914 mm long straight uniform 50 Ω microstrip lines with the DCL-launchers in GSM900 receive band at 2×43 dBm carrier power. All lines were manufactured in the same batch and coated by a 1 μm immersion tin finishing.

The nominal laminate, referred to as '100% PTFE bonding' in Fig. 1, is the commercial Taconic TLX-9 material (substrate thickness is 0.76 mm) that has a layer of pure PTFE at the substrate surface. The laminate has the relative permittivity $\varepsilon_r = 2.5$ and dissipation factor $\tan\delta = 0.0019$ at 10 GHz, according to the manufacturer's specification. The copper cladding is 35-μm thick low-profile drum-side treated (DST) copper foil attached by the treated side to the dielectric substrate. The treated side of the copper foils had a very thin commercial chromate passivation layer, which was not removed prior to lamination. The 1 μm immersion tin coating has been applied over the etched copper tracks to prevent copper oxidation.

The two materials with the modified interfaces are the following:

- The laminate, referred to as 'adhesion promotor' in Fig. 1, contains the inverted copper foil cladding, that is, the DST-copper foil is attached by the matte side to the substrate. The adhesion promotor is pre-applied to the copper underside, that is, to the side being attached to the substrate. The substrate parameters measured at 10 GHz are $\varepsilon_r = 2.56$ and $\tan\delta = 0.0015$.

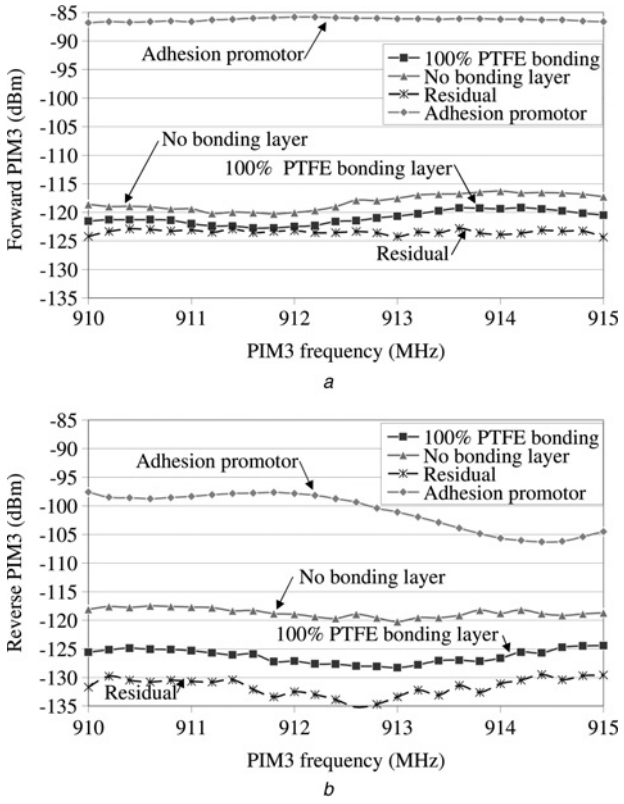

Figure 1 *Characterisation of the laminates with different conductor-to-substrate interfaces, viz., the nominal laminate with 100% PTFE bonding, the laminate with inverted copper cladding and adhesion promotor, and the laminate with no bonding layers and rearranged substrate plies. The measurements were carried out on 914 mm long straight uniform 50 Ω microstrip lines and the data present the mean values over a series of 3 reconnections of the test cables*

a Measured forward PIM3 products
b Measured reverse PIM3 products

• The laminate, referred to as 'no bonding layers' in Fig. 1, contains the same copper cladding as the nominal material but its fabric plies are rearranged in such an order that the bonding layers of pure PTFE are moved from the substrate surface and sandwiched between the inner layers of the PTFE-coated glass fabric. The dielectric substrate has the same thickness and electrical parameters as the nominal laminate.

The adhesion promotion is commonly used in PCB industry to facilitate interfacial adhesion of FR4-epoxy bonding plies to copper surfaces during lamination. It imparts a micro-etched surface along with an organo-metallic coating that enhances the foil to resin bonding [18]. However, in our study the adhesion promotor was employed in the PTFE-based laminate, and no chemical bonding was expected to develop due to the high chemical resistance of PTFE.

The measurement results in Fig. 1 show that the laminate with the adhesion promotion demonstrates noticeably higher forward and reverse PIM3 levels. It is noteworthy that the exposed substrate surface of the sample with the promotor-treated copper foil has nearly black colour, as opposed to the light brown colour of the nominal laminate surface in Fig. 2*a*. Such a dramatic change in the substrate surface colour indicates that the bond promotor either contains oxidised copper foil and the products of this reaction diffused into the molten PTFE bonding layer during the lamination process, or has had an effect on the crystallinity rate of the surface layers of PTFE. The former mechanism seems more plausible, and this conclusion is supported by the SEM images of Fig. 2*b*, which show flocculent structure of the promoter-treated foil in comparison with the original dendritic structure of the nominal copper foil surface in Fig. 2*c*. Anyway, the observed modification of the interface between copper foil and substrate proved to have direct correlation with the significantly higher measured PIM level.

The effect of rearranging the substrate layers is less pronounced, as compared with the adhesion promotion. Bearing in mind the estimated measurement uncertainty due to a single error source [19], one could suggest that the measured forward PIM3 levels of the nominal and modified laminates are barely different. But the measured reverse PIM3 levels clearly demonstrate higher PIM production in the modified substrate. It also stands out that in the modified laminate the reverse and forward PIM3 levels are nearly the same that might indicate the localised PIM generation [12]. The typical measurement uncertainty is in the range from +2.4 to −3.3 dB when the residual PIM level of the test setup is ∼10 dB below the measured PIM products of the device under test but it increases in the measurements closer to the residual level.

Inspection of the strip interface in Fig. 3 revealed that both the nominal and rearranged laminates exhibited fractured edge foot of the etched strips and a small area of contamination near the strip edge [20]. However, the modified laminate without the surface bonding layer displayed slightly stronger edge degradation. The contamination content included copper oxide, residual etchant and residues of the dissolved blue-film photoresist. Contamination and fracturing of the strip edges are deemed to be the primary causes of the distributed PIM generation, particularly due to considerably higher electric current density near the strip edges and at the strip bottom surface [21].

Moreover, contamination with chemicals and etchant residues has long been presumed as a cause of degradation of the electrical performance of printed circuits [22]. However, this is not the only interface factor, which determines the fluctuating PIM response, as will be discussed in next section.

doi: 10.1049/iet-map.2010.0070

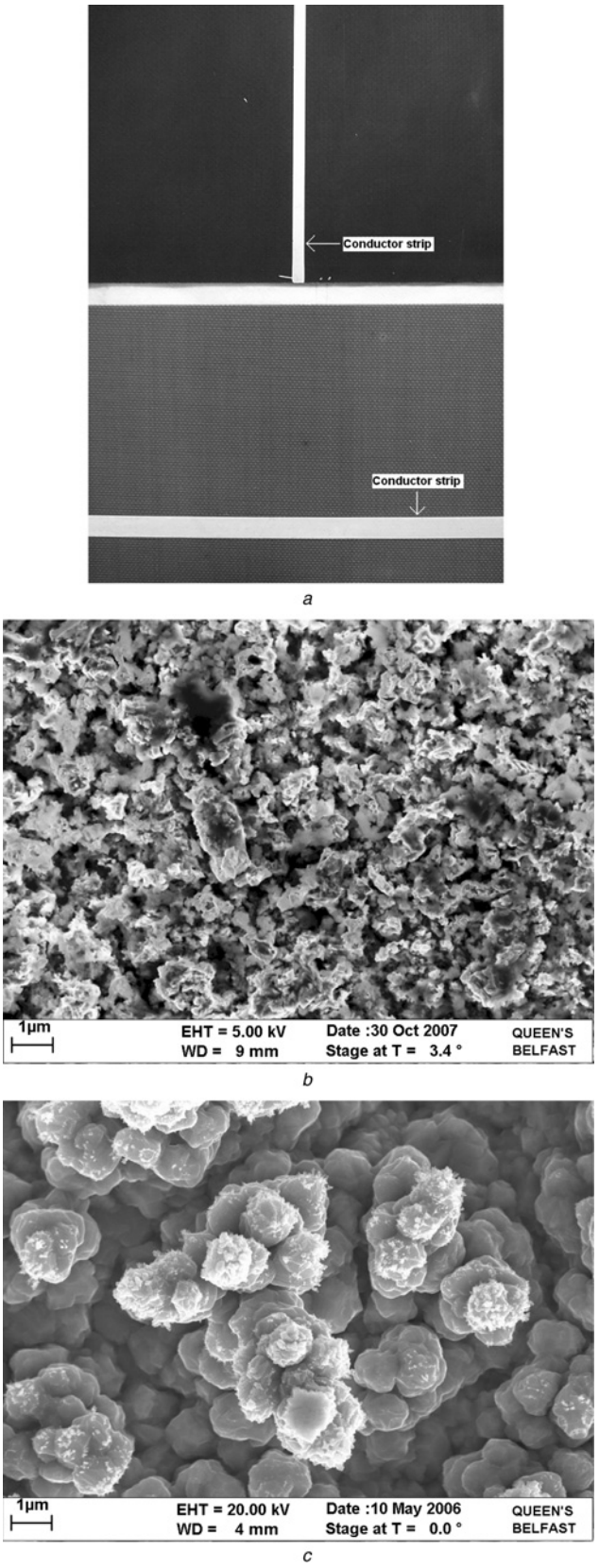

Figure 2 *SEM images of the interface side (underside)*

a Exposed substrate surface of the nominal (below) and promoter-modified (above) laminates with the sections of tin-plated strips
b Copper foil with the adhesion promotion treatment
c Nominal copper foil

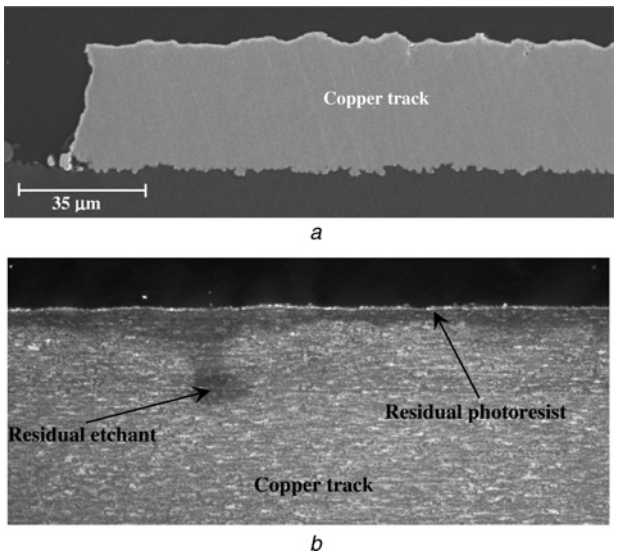

Figure 3 *Typical conditions at the strip edges on the processed nominal laminate [20]*

a Cross-sectional SEM view on the strip edge fracturing
b High-resolution optical microscopy of the edge contamination on the copper track underside

3 Long-term stability of PIM response

The long-term stability of the electrical performance is imperative for the high-performance applications of printed circuits. To our best knowledge, no systematic study of how PIM performance of the printed circuits varies over extended period of time has been reported in the technical literature. In order to explore this problem, the forward PIM3 level has been monitored on microstrip transmission lines with different finishing. Four replicas of microstrip lines were fabricated for each type of the finishing on the commercial Taconic RF-30 laminate with 0.76-mm thick substrate and 35 μm DST-copper cladding. Further details on the microstrip layouts for contactless test fixture can be found in [10, 11]. All the panels were processed in the same batch. The reference samples had bare copper tracks, while the conventional coatings of 1 μm immersion tin and solder mask over bare copper, further referred to as green mask, were applied to the other samples. The forward PIM3 measurements were performed on 1234 mm long microstrip lines with CSLs at single frequency of $f_{PIM3} = 915$ MHz ($f_1 = 930$ MHz, $f_2 = 945$ MHz) at 2×43 dBm carrier power. The specimens were tested at several instances during the 80-day period commencing from the shipping date. Between the test sessions the panels were stored on a flat surface in office environment.

Special attention was paid to evaluating the measurement uncertainty associated with consistency of the test conditions. Several series of tests were performed on different laminates, including Taconic RF-30 laminate with relatively high PIM level (from −70 down

to −110 dBm, depending on date the measurement was taken, as further discussed below) and a reference green-masked laminate with the PIM performance close to the residual PIM level of the test setup. The repeatability test involved replacing a printed board in the test fixture five times in a row. The maximum deviations of the PIM level measured with the same sample in this test were within ±1.2 dB, which provides the estimate of the experimental uncertainty due to replacing a printed board into the test fixture. Slightly higher experimental uncertainty was observed when the test took longer.

Other factors influencing PIM measurements were also studied. Those included the test board flatness and cleaning with micro-fibre cloth, water rinse and pressured air, which typically caused variations in the measured PIM level within approximately ±3 dB. The effect of laboratory environment, that is, ambient temperature and humidity, is believed to be less significant. Nevertheless, the precautions taken during the board storage and handling enabled us to limit the total experimental uncertainty to ±2 dB, which is applicable to all results presented below.

The measurement results in Fig. 4*a* demonstrate considerable improvement of the PIM3 performance of the bare copper and green-masked boards during the first period of 25 days. Notably, the bare copper tracks produce significantly higher PIM3 level which faster decreases over the test period as compared with the coated boards. The tin-plated boards exhibit much less variations of PIM3 level.

During the first two rounds of measurements, slight warping of the green-masked boards was observed, presumably due to the contraction of the coating film. At the third round of measurements, that is on the 7th-day after shipping, the panels were bent in order to make them flat. This resulted in significantly higher PIM production rate on two of four boards, which suggested another phenomenon involved. Therefore it was decided to repeat the bending experiment at several instances (26th and 49th days from the shipping date) on all boards with different finishing.

On the 26th- and 49th-day, each panel was bent in the same manner about a cylindrical post of diameter of 155 mm, Fig. 5, and held bent for approximately 5 s. Noticeably, the bending direction, either across or along the printed tracks, had no discernable effect on the line matching. However, a slight difference (less than 4 dB) in PIM3 levels was observed between the measurements after bending across and along the tracks. To square the test conditions and eliminate the uncertainty associated with the bending, each panel subjected to the PIM tests was bent in both directions at a time.

The measurement results in Fig. 4*b* demonstrate that the PIM3 levels on the tested panels gradually decrease until the panels are bent. Bending the panels resulted in considerable rise of the PIM3 production followed by its

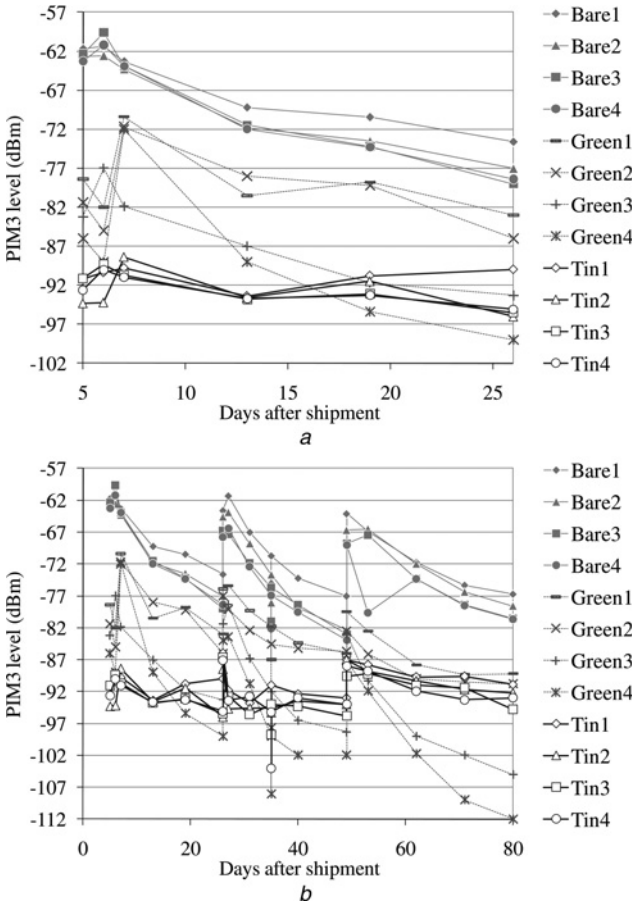

Figure 4 *Instability of the PIM3 response and the effect of panel bending measured on Taconic RF-30 laminate with different strip finishing (bare copper, green mask and immersion tin)*

a Self-determined PIM3 improvement during first period of 25 days after shipping

b Effect of the panel bending on 26th and 49th days after shipping

gradual decrease similar to that before bending. The rate of decrease is fairly the same within each group of the boards, but differs among the three groups. Tin-plated boards appear to be least sensitive to the panel bending and demonstrate the greatest stability of the PIM3 performance during the 26-day period.

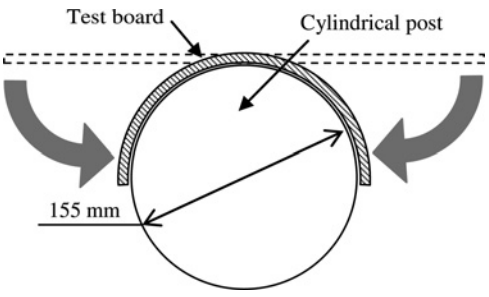

Figure 5 *Bending the laminate boards around the cylindrical post*

doi: 10.1049/iet-map.2010.0070

On the 35th day, the measurements were carried out using different position of the boards in the text fixture, viz., the specimens were placed into the test fixture upside down thus emulating an inverted microstrip line. A sheet of a laminate with copper foil completely removed from both sides was inserted as spacer between the test board and ground plane of the test fixture. It was suitably holed to apply the vacuum clamping. This test arrangement provided similar physical conditions at the spacer/fixture interface for different printed boards and thus could have allowed us to reduce the corresponding experimental uncertainty in comparative PIM testing. However, inverting the test boards had not been envisaged in the test fixture design and therefore inflicted significant modification of the measurement conditions, particularly, the port matching and microstrip losses. The latter changes entailed noticeably lower PIM level measured on the upside-down boards as compared with the conventional test arrangement. Namely, PIM level dropped by 4–5 dB on the bare copper, 0–13 dB on the green-masked and 0.7–9 dB on the tin-plated boards, while the corresponding return loss decreased from 13.8 to 7.8 dB on the bare copper and tin-plated boards and from 16.9 to 8.0 dB on the green-masked boards. The variations in PIM level have been attributed to the increased port reflection due to mismatch which resulted in less carrier power delivered to the line and standing-wave contribution to the distributed PIM production. While the former factor is self-explanatory, the latter contribution has no straightforward interpretation and still needs further investigation. The larger spread of data for the coated boards, as compared with the bare copper ones, might have been inflicted by the mechanical stress imposed on the coating due to vacuum clamping and therefore underlines the contribution of the printed strip coatings to the distributed PIM production.

The observed behaviour of the PIM performance could be attributed to the stress relaxation in the woven glass/PTFE composite substrates. The test fixture with CSLs employed in testing of PIM3 stability required that copper cladding be completely removed from the bottom side of the printed boards and most of the cladding be etched out at the top side during track routing. Indeed, so extensive etching inevitably causes dimensional instability of the substrate due to relaxation of the inherent stress imposed in the course of the glass fabric coating and panel lamination processes [23, 24]. In particular, the manufacturer specification [25] for RF-30 laminate states 200–400 ppm lengthwise (machine direction) expansion and up to 1000 ppm crosswise (cross direction) shrinkage as the typical estimates for stripped laminates. Similarly, bending of the boards is thought to have caused considerable elastic stretching strain and its subsequent relaxation after releasing the boards. The dimensional movement due to the viscous response of the amorphous phase of semi-crystalline PTFE can take days in ambient conditions, which seems to be consistent with the time scale of the variations observed in Fig. 4.

It is noteworthy that the stress relaxation can be facilitated at elevated temperatures. This phenomenon has entailed the weaker PIM3 response of the green-masked and tin-plated boards, because application of these coatings involves high-temperature processes. Furthermore, the green-mask coating on its own could inflict additional dimensional instability of the finished boards caused by the strain variations, which may be indicated by the larger spread of the PIM3 responses of the green-masked boards in Fig. 4.

Whatever are the actual physical phenomena underlying the effect of elastic stress relaxation in the processed PTFE-based substrates on PIM performance of the printed lines, they still need more detailed investigation. However, the following considerations can shed some light on the observed effects.

The electrostriction of PTFE has been reported as a mechanism of PIM production in coaxial cables at RF frequencies [26]. In printed circuits, respectively, there are several factors which draw close attention to the electrostriction phenomenon. Namely, the etched PTFE surface is inherently porous, owing to indentations caused by the dendrites at the copper foil underside imprinted during the lamination. Open-porous PTFE films demonstrate noticeable electrostriction, subject to the degree of porosity [27]. As a result of the electrostriction, electric displacement in porous PTFE films appears to be a non-linear function of applied electric field [28] with quite a strong measured non-linear response at low frequencies [27]. Indeed, stretching the PTFE films increases their porosity and vice versa. Therefore one may hypothesise that the shrinkage of the porous PTFE surface of the boards after etching out most of the copper cladding could contribute to the PIM3 level decrease observed in Fig. 4.

To gain deeper insight into the mechanisms of the long-term stability of the PIM response in commercial laminates, a series of PIM tests has been performed on Taconic TLX-8 laminate with 0.76-mm thick substrate and 35 μm DST-copper cladding. Two printed line specimens were fabricated for each of the bare copper, green-mask and tin-plated finish coatings. All the boards were processed by the same manufacturer.

The general trends in Fig. 6 appear to be similar to those in Fig. 4, although there are several distinctive features to note. First, the tin-plated boards demonstrate considerable improvement of their PIM performance over time, as contrasted with the stable PIM response measured on the tin-plated boards of Taconic RF-30 laminate in Fig. 4. Secondly, one can infer from Fig. 6 that each bending of the bare copper and tin-plated boards on the 26th and

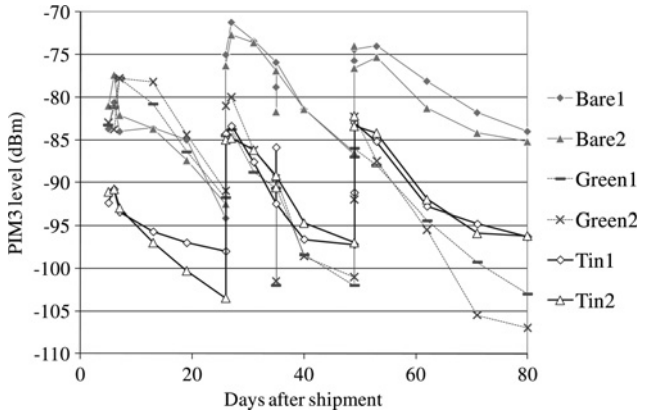

Figure 6 *Variations of the PIM3 response and the effect of panel bending on 26th and 49th days after shipping measured with the processed printed lines on Taconic TLX-8 laminate with different strip finishing (bare copper, green mask and immersion tin)*

49th days inflicted some irreversible changes, which are indicated by the gradual increase of the remnant PIM level before bending on the 49th and 80th days. Conversely, the green-masked boards in Fig. 6 demonstrate the steady improvement perturbed only by the bending actions, similar to those in Fig. 4.

Thirdly, the overall PIM3 level measured on the bare copper boards in the first tests appears to be 20 dB higher for the Taconic RF-30 material as compared with the Taconic TLX-8 laminate, see Figs. 4 and 6. Furthermore, the PIM3 level measured on all RF-30 boards remains slightly higher than that on the corresponding boards of the TLX-8 laminate over whole monitoring period.

Similar to the RF-30 boards, most of the TLX-8 boards demonstrated decreased PIM level on day 35 when being turned upside-down, and the return loss changed from 13.4 to 7.3 dB on the bare copper and tin-plated boards and from 17.0 to 7.7 dB on the green-masked boards.

Although both RF-30 and TLX-8 materials contain the same base dielectric and copper cladding, their glass fabric plies are slightly different. Also, the substrate of the RF-30 laminate contains the inner PTFE-coated glass fabric plies densely filled with ceramic nanospheres, whereas the glass fabric plies of the TLX-8 substrate are coated by pure PTFE. The filler particles, even being made of a linear non-ferroic material, apparently increase the porosity of the PTFE coating and thus may inflict detectable impact on the PIM production rate.

It is also noteworthy that the bare copper tracks on RF-30 laminate in Fig. 4 exhibit the higher PIM level than the coated tracks. One may reasonably argue that this could be simply a result of initial oxidation of the pre-processed copper foil or environmental oxidation of the processed copper tracks. The residual copper oxides are removed in the course of microetching used to pre-clean the copper tracks before applying the finish coating, which makes the coated lines virtually free of the oxidation and protected against environmental effect.

However, the observed overall improvement of PIM level on the bare tracks is inconsistent with degradation of the PIM performance of the printed lines due to growing copper oxide, as demonstrated in Section 2. Also, the similar trends in self-improved PIM performance of bare and coated tracks on both RF-30 and TLX-8 laminates suggest that the age-inflicted oxidation has minor effect on the PIM performance of bare copper tracks. Therefore it seems unlikely that the copper oxide content increased during the 80-day storage and noticeably affected the PIM performance of the bare copper boards.

Let us also note that, according to the manufacturer specification, both RF-30 and TLX-8 laminate materials had similar typical estimates for the dimensional variations. Therefore assuming the observed PIM3 improvement to be caused by the dimensional changes, one may expect the rates of PIM3 level decrease for both laminate materials to be correlated. The results for the bare copper and green-mask boards presented in Figs. 4 and 6 proved to be consistent with this expectation.

Finally, Fig. 7 shows the results of PIM3 characterisation of the prospective Taconic LCAM laminate with 0.84-mm thick substrate, 35 μm DST-copper foil cladding and tin-plated microstrip lines. As distinct from the previous materials, LCAM laminate substrate contains ceramic-filler-loaded epoxy coating of the glass fabric plies. It appears that, in spite of slight changes inflicted by the panel bending on 26th and 49th days after shipment, the boards show no conclusive evidences of PIM3 variations. The overall stability of the PIM3 level measured on the LCAM material could indicate a possible ameliorative effect of the epoxy coating on the dimensional stability and thus on the PIM performance of the laminate.

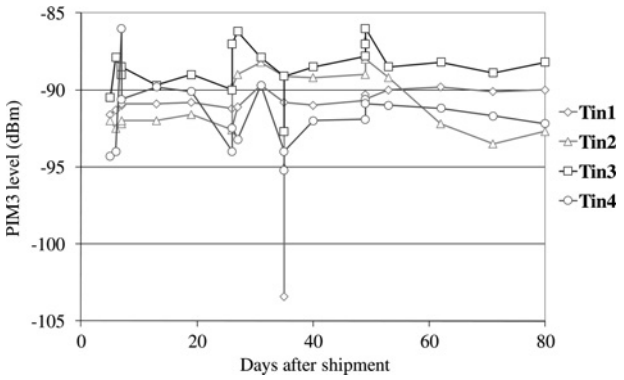

Figure 7 *PIM3 response and the effect of panel bending on 26th and 49th days after shipping measured with the processed printed lines on Taconic LCAM laminate with immersion tin finishing*

IET Microw. Antennas Propag., 2011, Vol. 5, Iss. 1, pp. 68–76
doi: 10.1049/iet-map.2010.0070

The PIM level in the LCAM boards decreased by 1–13 dB when the boards were placed upside-down into the test fixture on day 35, while the return loss changed from 19.3 to 9.2 dB. The observed PIM level decrease is fully consistent with the corresponding results on RF-30 and TLX-8 boards. Thus, the presented results provide the first indication of the stress relaxation phenomenon involved in the PIM production in the studied PTFE-based laminates. It should, however, be appreciated that the underlying microscopic mechanisms of the self-improvement of PIM performance, as well as the origins of the distributed non-linearity in tested printed lines, still require further thorough investigation.

4 Conclusions

The presented experimental observations demonstrate the key role of the conductor-to-substrate interface in distributed PIM generation. It has been shown that the commercial adhesion promotion considerably increases the undesired PIM generation in microstrip lines. In contrast to the impractical PTFE-based laminate with the adhesion promotion applied in our study, the bond promotor in the commercial epoxy-based laminates provides chemical bonding between the copper foil and resin substrate. The by-products of the chemical binding could deteriorate the PIM performance of the printed lines, which has been observed in our study.

It has also been shown that removing the bonding layers from the substrate surface results in higher PIM production rate. This effect has been attributed to the strip edge delamination and subsequent trapping of the chemicals and etchant residues. The PIM performance improvement over a long-term period has been experimentally observed on microstrip lines with different finish coating. It has been demonstrated that the bending of processed boards causes dramatic increase of the PIM level which gradually decreases to the initial PIM level in the flat board after releasing from bending. These phenomena have been attributed to the elastic stress relaxation in the processed and bent PCB panels and/or to a chemical reaction of the residues trapped at the strip edges. However, the understanding of microscopic mechanisms behind the long-term variations of PIM performance of printed circuits still requires further corroboration.

5 Acknowledgments

The authors are grateful to Taconic Advanced Dielectric Division Ltd, Trackwise Designs Ltd, PCTEL Inc. and Castle Microwave Ltd for providing with the test samples and measurement facilities. Special thanks go to Mr M. Huschka of Taconic ADD Ltd for his continuous support and particularly for his valuable advice on this paper, to Mr N. Carroll for his help with the measurements and to Professor R. Bowman of the Centre for Nanostructured Media, Queen's University of Belfast for his assistance with SEM imaging of the copper foil samples.

6 References

[1] ARAI H.: 'Outdoor and indoor cellular/personal handy phone system base station antenna in Japan', GODARA L.C. (ED.): 'Handbook of antennas in wireless communications' (CRC Press, 2001), Chapter 11, pp. 1–26

[2] BAO VU T.: 'Smart antenna system architecture and hardware implementation', in GODARA L.C. (ED.): 'Handbook of antennas in wireless communications' (CRC Press, 2001), Chapter 22, pp. 1–32

[3] HUANG J.: 'Microstrip antennas: analysis, design and application', in BALANIS C.A. (ED.): 'Modern antenna handbook' (Wiley, Tempe, Arizona, 2008), pp. 157–200

[4] SOLBACH K., BÖCK M.: 'Intermodulation in active receive antennas'. Proc. German Radar Symp., Bonn, Germany, 2002

[5] PASCHOS G.S., KOTSOPOULOS S.A., ZOGAS D.A., KARAGIANNIDIS G.K.: 'The impact of intermodulation interference in superposed 2 G and 3 G wireless networks and optimization issues of the systems provided QoS'. Proc. Int. Conf. on Computer, Communication and Control Technologies, Orlando, FL, 2003

[6] BUTLER R., KUROCHKIN A., HUGH N.: 'Intermodulation products of LTE and 2 G signals in multitechnology RF paths', *Bechtel Commun. Tech. J.*, 2009, **2**, (1), pp. 1–11

[7] ETSI EN 300 910: 'Digital cellular telecommunications system (Phase 2+); Radio transmission and reception', v8.5.1 (2000–11), 1999

[8] BARKLEY K.: 'Two-tone IMD measurement techniques', *RF Des. Mag.*, 2001, pp. 36–52

[9] SCHUCHINSKY A.G., FRANCEY J., FUSCO V.F.: 'Distributed sources of passive intermodulation on printed lines'. Proc. IEEE Antennas and Propagation Society Int. Symp., Washington, DC, July 2005, vol. 4B, pp. 447–450

[10] PÉREZ J.V.S., ROMERO F.G., RÖNNOW D., SÖDERBÄRG A., OLSSON T.: 'A microstrip passive intermodulation test set-up; comparison of leaded and lead-free solders and conductor finishing'. Proc. Fifth Int. Workshop on Multipactor, Corona and Passive Intermodulation, Noordwijk, The Netherlands, 2005, pp. 215–222

[11] EL BANNA B., OLSSON T., UDDIN J.: 'Sources of passive intermodulation in base station antenna systems'. Proc. Loughborough Antennas and Propagation Conf., Loughborough, UK, 2006, pp. 139–144

[12] SHITVOV A.P., ZELENCHUK D.E., SCHUCHINSKY A.G., FUSCO V.F.: 'Passive intermodulation generation on printed lines: near-field probing and observations', *IEEE Trans. Microw. Theory Tech.*, 2008, **56**, (12), Part 2, pp. 3121–3128

[13] SHITVOV A.P., ZELENCHUK D.E., SCHUCHINSKY A.G., FUSCO V.F.: 'Passive intermodulation in printed lines: effects of trace dimensions and substrate', *IET Microw. Antennas Propag.*, 2009, **3**, (2), pp. 260–268

[14] ZELENCHUK D.E., SHITVOV A.P., SCHUCHINSKY A.G., FUSCO V.F.: 'Discrimination of passive intermodulation sources on microstrip lines'. Proc. Sixth Int. Workshop on Multipactor, Corona and Passive intermodulation in Space RF Hardware, Valencia, Spain, 2008, pp. 1–4

[15] ZELENCHUK D.E., SHITVOV A.P., SCHUCHINSKY A.G.: 'Effect of laminate properties on passive intermodulation generation'. Proc. Loughborough Antennas and Propagation Conf., Loughborough, UK, 2007, pp. 169–172

[16] FRANCEY J.: 'Passive intermodulation study'. Taconic ADD, Technical Report, 2002

[17] SHITVOV A.P., ZELENCHUK D.E., OLSSON T., SCHUCHINSKY A.G., FUSCO V.F.: 'Transmission/reflection measurement and near-field mapping techniques for passive intermodulation characterisation of printed lines'. Proc. Sixth Int. Workshop on Multipactor, Corona and Passive Intermodulation in Space RF Hardware, Valencia, Spain, 2008, pp. 1–6

[18] LIN W., LIN D., HSU K., CHANG K.S., CHU C.: 'The use of modified oxide process for lead-free application'. Proc. Int. Microsystems, Packaging, Assembly and Circuits Technology Conf., 2007, pp. 234–237

[19] 'Summitek instruments passive IM analyzer system: operating and maintenance manual'. Summitek Instruments Inc., Part Number 1902000, June 2004

[20] 'Assessment of PTFE based PCB laminates for interface condition'. MCS Ltd, Report No. 20002-01425(fv1), May 2007

[21] HOFFMANN R.: 'Handbook of microwave integrated circuits' (Artech House, Norwood, MA, 1987)

[22] TRAUT G.R.: 'Advances in substrate technology', in JAMES J.R., HALL P.S. (ED.): 'Handbook of microstrip antennas' (Peter Peregrinus Ltd., 1989), vol. 2, pp. 871–956

[23] 'Taconic fastRise27 multilayers general processing guidelines'. Taconic Advanced Dielectrics Division

[24] 'After Etch stress relief in RT/duroid® high frequency laminates'. Advanced Circuit Materials Division, Rogers Corporation, Fabrication Guidelines 4.2.2, Publication #92-422, 2003

[25] 'ORCER RF-30'. Taconic Advanced Dielectrics Division, Technical Datasheet, November 2007

[26] HELME B.G.M.: 'Passive intermodulation of ICT components'. Proc. IEE Colloquium on Screening Effectiveness Measurements, London, UK, May 1998, pp. 1–8

[27] SCHWÖDIAUER R., NEUGSCHWANDTNER G., BAUER-GOGONEA S., BAUER S., HEITZ J., BÄUERLE D.: 'Dielectric and electret properties of novel Teflon PTFE and PTFE-like polymers'. Proc. Tenth Int. Symp. on Electrets, Delphi, Greece, 1999, pp. 313–316

[28] FURUKAWA T., MATSUMOTO K.: 'Nonlinear dielectric relaxation spectra of polyvinyl acetate', *Jpn. J. Appl. Phys.*, 1992, **31**, (3), Part 1, pp. 840–845

doi: 10.1049/iet-map.2010.0070